Robust sparse reconstruction for Cherenkov luminescence tomography based on look ahead orthogonal matching pursuit algorithm

Cai, Meishan, Zhang, Zeyu, Hu, Zhenhua, Tian, Jie

Meishan Cai, Zeyu Zhang, Zhenhua Hu, Jie Tian, "Robust sparse reconstruction for Cherenkov luminescence tomography based on look ahead orthogonal matching pursuit algorithm," Proc. SPIE 10871, Multimodal Biomedical Imaging XIV, 1087114 (27 February 2019); doi: 10.1117/12.2509062

SPIE.

Event: SPIE BiOS, 2019, San Francisco, California, United States

Robust sparse reconstruction for Cherenkov luminescence tomography based on look ahead orthogonal matching pursuit algorithm

Meishan Cai[a, b], Zeyu Zhang[a, c], Zhenhua Hu[a, b], Jie Tian[a, b, c, *]
[a]Key Laboratory of Molecular Imaging, Institute of Automation, Chinese Academy of Sciences, Beijing 100190, China
[b]University of Chinese Academy of Sciences, Beijing 100049, China
[c]School of Life Science and Technology, Xidian University, Xi'an, Shaanxi 710071, China

ABSTRACT

Cherenkov luminescence tomography (CLT) has become a novel three-dimensional (3D) non-invasive technology for biomedical applications such as tumor detection, pharmacodynamics evaluation, etc. However, the reconstruction of CLT still remains a challenging task because of the strong absorbing effect and scattering effect of Cherenkov photon transport process. In this study, we proposed a novel robust sparse reconstruction method named look ahead orthogonal matching pursuit (LAOMP) algorithm to improve the robustness and accuracy of reconstruction for CLT instead of traditional OMP algorithm based on a look ahead strategy. To validate the reconstruction performance of LAOMP method, a series of numerical simulations were conducted. The results showed that LAOMP method obtained the higher robustness and accuracy in locating the optical sources compared with the OMP and StOMP algorithms.

Keywords: Cherenkov luminescence tomography (CLT), orthogonal matching pursuit (OMP), look ahead orthogonal matching pursuit (LAOMP), sparse reconstruction, tumor detection

1. INTRODUCTION

Cherenkov radiation is produced when high-energy charged particles pass through a medium at a speed faster than the speed of light in the medium. [1] This effect is used as optical molecular imaging first in 2009, as a new imaging modality called Cherenkov luminescence imaging (CLI). [2] CLI has many advantages, including high spatial resolution, low costs and available clinical radiopharmaceuticals used for positron emission tomography (PET) or single-photon emission computed tomography (SPECT) such as ^{18}F, ^{11}C, ^{64}Cu, ^{131}I. [3-4] However, 3D distribution of radioactive probes remains unknown because CLI is a planar imaging technology which can only provide the surface light flux information of targeted tissue. [5]

Combined with structural imaging modality, CLI technology is extended to 3D tomography by many research groups, named as Cherenkov luminescence tomography (CLT), which can provide more accurate spatial distribution information of radionuclides in biological tissues for preclinical and clinical researches. [6-8] Since CLT combines the advantages of optical imaging and radionuclide imaging, it can be used as a low-cost substitute of PET scan. However, like other optical molecular imaging modality such as bioluminescence tomography (BLT) and fluorescence molecular tomography (FMT), the inverse problem of CLT is greatly ill-conditioned and ill-posed because of the strong absorbing effect and scattering effect of photon in the biological tissues. On the other hand, strong noise interference exists in the reconstruction process of CLT, which requires highly robust reconstruction algorithm. To acquire more accurate and robust reconstruction of CLT, it is important to employ the prior information such as weighted multi-spectrum strategy [9], sparse regularization [10] and so on. However, Tikhonov regularization, the most wildly used method in the inverse problem, will bring in many pseudo sources, known as over-smoothed problem.

Matching pursuit algorithm is a kind of fast sparse reconstruction algorithm, which is wildly used in optical molecular tomography. For reconstruction of CLT, Liu et al. propose preconditioning orthogonal matching pursuit (POMP) modified from traditional matching pursuit algorithm and acquire better reconstruction performance. [11] However, these algorithm still have insufficient accuracy and robustness. In this study, a novel robust reconstruction algorithm called look ahead orthogonal matching pursuit (LAOMP) was proposed for CLT reconstruction. Look ahead strategy was used to improve

Multimodal Biomedical Imaging XIV, edited by Fred S. Azar, Xavier Intes, Qianqian Fang, Proc. of SPIE
Vol. 10871, 1087114 · © 2019 SPIE · CCC code: 1605-7422/19/$18 · doi: 10.1117/12.2509062

the robustness and accuracy of orthogonal matching pursuit for reconstruction of CLT. Numerical simulation experiments were conducted to validate the reconstruction performance of LAOMP algorithm. The results demonstrated that LAOMP algorithm had better location accuracy and robustness for reconstruction of CLT compared to other matching pursuit algorithms such as orthogonal matching pursuit (OMP) and stage-wise orthogonal matching pursuit (StOMP).

2. METHODS

2.1 Photon transmission model and inverse problem

Generally, without considering the influence of time, the steady-state radiation transfer equation (RTE) is used to mimic the transmission process of photons in biological tissues. However, it is too difficult to solve the steady-state RTE directly because of the coupling of direction and position of the solid angle. Based on spherical harmonic function theory, the steady-state RTE can be approximately simplified to diffusion equation by the first order spherical harmonic function. Joint the boundary condition, the diffusion equation can be formulated as [12]

$$\begin{cases} -\nabla[D(r)\cdot\nabla\Phi(\mathrm{r})]+\mu_a(r)\cdot\Phi(\mathrm{r})=S(r) \\ \Phi(\mathrm{r})+2A(n)\big(v(r)\cdot D(r)\big)=0,\ \ r\in\partial\Omega \end{cases} \quad (2\text{-}1)$$

Where ∇, r Ω, $\partial\Omega$ denote the vector differential operator, position coordinate, biological tissues and the surface of biological tissues respectively. $\Phi(\mathrm{r})$ is the light flux at position $r\in\Omega$. $S(r)$ is the isotropic source radionuclide distribution, and $D(r)$ is the optical diffusion coefficient defined as

$$\mathrm{D(r)}=\frac{1}{3(\mu_a(r)+(1-g)\cdot\mu_s(r))} \quad (2\text{-}2)$$

Where $\mu_a(r)$ represents light absorbing coefficient, g is the medium anisotropy factor, $\mu_s(r)$ is light scattering coefficient. $\mu_s'(r)=(1-g)\cdot\mu_s(r)$ is also known as the reduced scattering coefficient. The continuous DE model must be discretized for numerical implementation on the computer. In practical terms, the finite element method (FEM) framework is often applied for the discretization of DE model in CLT such that DE model can be depicted as a system of linear equations as follows

$$\mathrm{Ax}=\mathrm{b} \quad (2\text{-}3)$$

Where A is the photon transmission systematic matrix, x is the optical density distribution of radionuclide, and b is the light flux at the boundary. In numerical simulation experiments or in vivo experiments, the light flux at the boundary b can be measured by optical signal acquisition device and the systematic matrix is calculated according to the heterogeneous structural mesh and optical coefficients such as absorbing coefficient, scattering coefficient and anisotropy factor. The inverse problem is to solve optical density distribution x after knowing the systematic matrix and the light flux at the boundary. Because the number of rows in matrix A is less than the number of columns, Eq. (3) is underdetermined. Therefore, sparse prior is usually adapted for solving the inverse problem, formulated as follows

$$\begin{cases} min\|x\|_0 \\ \|Ax-b\|_2<\varepsilon \end{cases} \quad (2\text{-}4)$$

Where $\|x\|_p$ denotes p-norm of x, ε is a relatively small quantity.

2.2 Look ahead orthogonal matching pursuit

To apply orthogonal matching pursuit algorithm for solving the inverse problem of CLT, Eq. (3) is normalized by bringing in the diagonal matrix Λ, where the i-th element of Λ is set as

$$\Lambda_i=\frac{1}{\|A_i\|_2^2} \quad (2\text{-}5)$$

Then we can transform Eq. (3) as follows

$$\begin{gathered} Ny=b \\ N=A\Lambda \\ y=\Lambda^{-1}x \end{gathered} \quad (2\text{-}6)$$

Hence, the inverse problem of CLT can be redefined as

$$\begin{cases} min\|y\|_0 \\ \|Ny-b\|_2<\varepsilon \end{cases} \quad (2\text{-}7)$$

$$x = \Lambda y$$

Since the problem is NP-hard problem, it is too difficult to find the exact solution with traditional optimization methods. Herein, OMP algorithm can be used as a kind of greedy algorithm to find the approximate solution. Firstly, we define the residual vector as

$$r_k = b - N_{I_k} y_{I_k} \quad (2\text{-}8)$$

Where I_k is the support set which contains the index of the selected column. The residual vector and the support set are initialed as

$$\begin{aligned} r_0 &= b \\ I_k &= \emptyset \end{aligned} \quad (2\text{-}9)$$

In each iteration, the OMP algorithm finds the column of *N* that is maximally correlated to the regularized residual vector, formulated as

$$\begin{aligned} i_k &= arg\ max_{(j \in (U - I_{k-1}))} dot(N_j, r_{k-1}) \\ I_k &= I_{k-1} \cup i_k \end{aligned} \quad (2\text{-}10)$$

Where U denotes the index of all column, *dot(a, b)* represents the inner product of *a* and *b*. The iteration stops when the number of elements in the support set reaches the sparsity level. In fact, The OMP suffers from the obvious drawback that one a particular column has been selected from the highest amplitude value of the matched filter, there is no way it can be removed. Therefore, the wrong columns are probable to be selected in the support set, which results in the reconstruction error correspondingly. The LAOMP algorithm is similar to the OMP algorithm in the fact that they both establish the support set by every iteration. However, the LAOMP algorithm takes into account the effect of adding that the selected column to the current support set on the final reconstruction accuracy by using the look ahead residue function. The lower residue means a better reconstruction performance in the view of the LAOMP method. [13] In each iteration, *L* highest amplitude components of the inner product of *N* and the residue vector *r* are put into the temp set

$$T_k = \max(dot(N_{U - I_{k-1}}, r_{k-1}), L) \quad (2\text{-}11)$$

Where T_k is the temp set in the k-th iteration, and max(N, L) means seeking the *L* largest elements in the vector *N*. All the elements in the support set are put into the look ahead residue function to calculate the final residues after *K* (sparsity level) iterations for selecting the best element, represented as

$$\begin{aligned} i_k &= arg\ min_{j \in T_{k-1}} (Look\_ahead\_residue(N_j)) \\ I_k &= I_{k-1} \cup i_k \end{aligned} \quad (2\text{-}12)$$

The process of calculating the final residue in the look ahead residue function is similar to the OMP algorithm. Therefore, the LAOMP algorithm for CLT can be summarized as Algorithm 1.

Algorithm 1.

Step 1. Input the surface light flux *b* and the systematic matrix *A*

Step 2. Normalize the systematic matrix by diagonal matrix Λ

$$Ny = b, N = A\Lambda, y = \Lambda^{-1}x$$

Step 3. Initial $y_0 = 0$, $r_0 = b$, $I_0 = \emptyset$, $U = range\left(1,\ col(N)\right)$, $k = 0$

Step 4. Repeat

$k = k + 1$

$T_k = \max(dot\left(N_{U-I_{k-1}}, r_{k-1}\right), L)$

$i_k = arg\ min_{j \in T_k}(Look\_ahead\_residue(N_j))$

$I_k = I_{k-1} \cup i_k$

Until $k > K$

Step 5. Calculate $y = N_{I_k}^{+} b$, $x^* = \Lambda N_{I_k}^{+} b$

Step 6. Output x^*

3. EXPERIMENTS AND RESULTS

In order to validate the reconstruction performance of the LAOMP algorithm, a series of simulation experiments were conducted. The digital mouse model was employed in the numerical simulation experiments. As the optical source was set at the abdomen part, about 30mm of trunk was cut off from the digital mouse. As a heterogeneous model, the trunk was divided into seven tissues manually according to the threshold of voxel, including bone, heart, stomach, liver, kidney, lung, muscle. At the wavelength of 650nm, the medium anisotropy factor g, the light absorbing coefficient $\mu_a(r)$ and the reduced light scattering coefficient $\mu_s'(r)$ of different tissues were listed in Table 1.

Table 1. Optical coefficient of different tissues at the wavelength of 650nm

Organs	**g**	$\mu_a(r)(mm^{-1})$	$\mu_s'(r)(mm^{-1})$
Bone	0.93	0.0017	1.1930
Heart	0.90	0.0080	1.0066
Stomach	0.93	0.0254	1.4798
Liver	0.93	0.0473	0.7000
Kidney	0.90	0.0090	2.3585
Lung	0.93	0.0265	2.2091
Muscle	0.97	0.0118	0.4674

A spherical shape Cherenkov source with radius 0.5mm was set at the center $(9.0\text{mm}, 20.0\text{mm}, 13.0\text{mm})$ inside the liver and the intensity of source was set to $1nw$ (Figure 1(a)). Then a mesh with 15824 nodes and 85029 tetrahedrons was generated from the heterogeneous trunk of digital mouse by Amira 5.2 (Figure 1(b)). With the optical coefficients and the generated mesh, the systematic matrix can be calculated by finite element method and the surface light flux was calculated by Monte Carlo method with MOSE v2.1 developed by our lab (Figure 1(c)). [14]

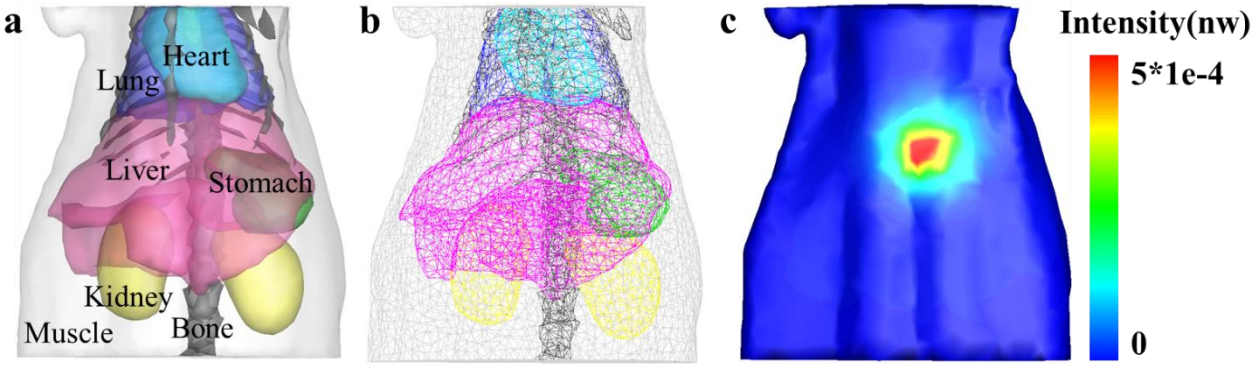

Figure 1. The results of the forward process with the digital mouse model. (a) The trunk part of heterogeneous digital mouse divided into seven different tissues, (b) the mesh generated from the trunk and (c) the surface light flux.

Based on the systematic matrix and the surface light flux obtained by MC simulation, the LAOMP algorithm was used to solve the inverse problem and reconstruct the optical source for CLT. At the same time, OMP algorithm and StOMP algorithm were conducted to reconstruct the optical source as the contrast group. The reconstructed results were shown in Figure 3. The slice at axis Z=13.0mm was selected to show the results of different algorithm. The true source was displayed with the white cycle (Figure 2(a)). Figure 2(c)-(d) were the reconstructed results by LAOMP algorithm, OMP algorithm and StOMP algorithm respectively. It showed that the result of LAOMP algorithm had the most similar position and shape with the true source compared with other two method.

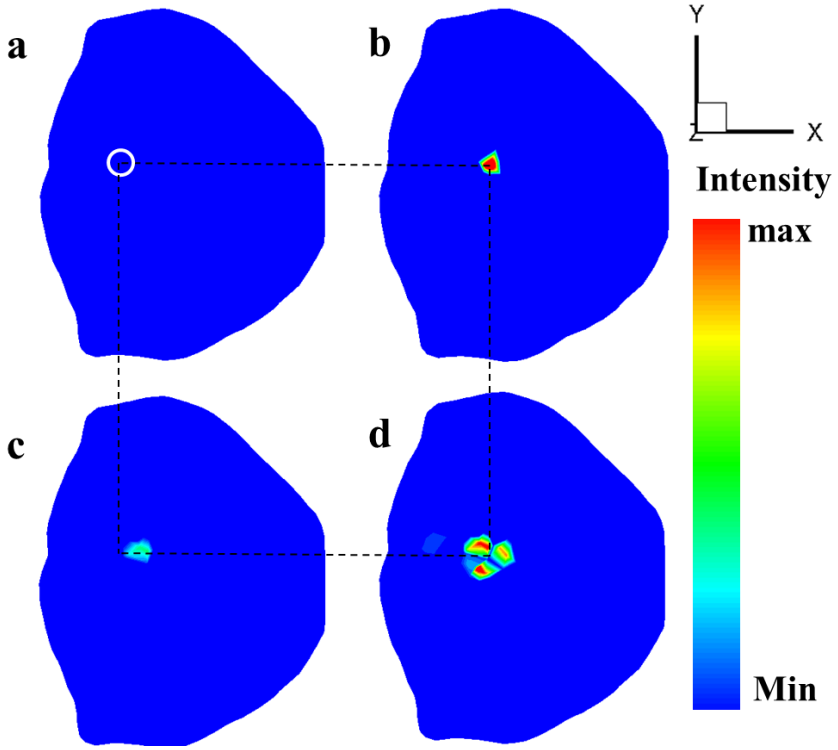

Figure 2. Reconstruction results of different algorithm. (a) The true source, (b) the results of LAOMP algorithm, (c) the results of OMP algorithm and (d) the results of StOMP.

4. DISCUSSION AND CONCLUSIONS

In this study, a novel algorithm named LAOMP algorithm was proposed to solve the inverse problem of CLT reconstruction. Compared with OMP algorithm and StOMP algorithm, proposed method selected the column more in a more cautious way by the look ahead strategy and obtained more accurate and robust reconstruction for CLT. Meanwhile, the shape could also be restored well according to LAOMP algorithm. It is believed that LAOMP can replace other OMPs as the fast reconstruction algorithm for CLT.

5. ACKNOWLEDGMENTS

This study was supported by the National Key Research and Development Program of China (2016YFC0102600, 2017YFA0205200), the National Natural Science Foundation of China (NSFC) (81227901, 81527805, 61622117, 81671759), the Beijing Nova Program (Z181100006218046), the Scientific Instrument Developing Project of the Chinese Academy of Sciences (YZ201672), and Chinese Academy of Sciences under Grant No. GJJSTD20170004.

REFERENCES

[1] Cerenkov, P. A. (1934). Visible luminescence of pure liquids under action of γ-radiation. Dok. Aka. Nau.(USSR), 2, 451-454.
[2] Robertson, R., Germanos, M. S., Li, C., Mitchell, G. S., Cherry, S. R., & Silva, M. D. (2009). Optical imaging of Cerenkov light generation from positron-emitting radiotracers. Physics in Medicine & Biology, 54(16), N355.
[3] Thorek, D. L., Robertson, R., Bacchus, W. A., Hahn, J., Rothberg, J., Beattie, B. J., & Grimm, J. (2012). Cerenkov imaging-a new modality for molecular imaging. American journal of nuclear medicine and molecular imaging, 2(2), 163.
[4] Boschi, F., & E Spinelli, A. (2014). Cerenkov luminescence imaging at a glance. Current Molecular Imaging, 3(2), 106-117.
[5] Li, C., Mitchell, G. S., & Cherry, S. R. (2010). Cerenkov luminescence tomography for small-animal imaging. Optics letters, 35(7), 1109-1111.
[6] Zhong, J., Tian, J., Yang, X., & Qin, C. (2011). Whole-body Cerenkov luminescence tomography with the finite element SP3 method. Annals of biomedical engineering, 39(6), 1728-1735.
[7] Hu, Z., Liang, J., Yang, W., Fan, W., Li, C., Ma, X. & Wang, J. (2010). Experimental Cerenkov luminescence tomography of the mouse model with SPECT imaging validation. Optics express, 18(24), 24441-24450.
[8] Spinelli, A. E., Kuo, C., Rice, B. W., Calandrino, R., Marzola, P., Sbarbati, A., & Boschi, F. (2011). Multispectral Cerenkov luminescence tomography for small animal optical imaging. Optics express, 19(13), 12605-12618.
[9] Guo, H., He, X., Liu, M., Zhang, Z., Hu, Z., & Tian, J. (2017). Weight multispectral reconstruction strategy for enhanced reconstruction accuracy and stability with Cerenkov Luminescence Tomography. IEEE transactions on medical imaging, 36(6), 1337-1346.
[10] Guo, H., Hu, Z., He, X., Zhang, X., Liu, M., Zhang, Z. & Tian, J. (2017). Non-convex sparse regularization approach framework for high multiple-source resolution in Cerenkov luminescence tomography. Optics Express, 25(23), 28068-28085.
[11] Liu, H., Hu, Z., Wang, K., Tian, J., & Yang, X. (2015, March). Cerenkov luminescence tomography based on preconditioning orthogonal matching pursuit. Medical Imaging 2015: Image Processing. International Society for Optics and Photonics, 2015, 9413: 94131X.
[12] Cong, W., Wang, G., Kumar, D., Liu, Y., Jiang, M., Wang, L. V., & Cong, A. (2005). Practical reconstruction method for bioluminescence tomography. Optics Express, 13(18), 6756-6771.
[13] Swamy, P. B., Ambat, S. K., Chatterjee, S., & Hari, K. V. S. (2014, February). Reduced look ahead orthogonal matching pursuit. In Communications (NCC), 2014 Twentieth National Conference on (pp. 1-6). IEEE.
[14] Tian, J., Liang, J., Chen, X., and Qu, X., “Molecular optical simulation environment," [M]//Molecular Imaging. Springer, Berlin, Heidelberg, 2013: 15-46.